

C-11 AN ALIAS PROTECTION SCHEME FOR RADON TRANSFORM

MICHAEL DENISOV and DMITRI FINIKOV

Geotechsystem, Ordzhonikidze 13/2, Moscow 117071, Russia

Summary

A variety of methods for seismic data processing based on the Radon decomposition are currently widely used in the industry. Due to finite spatial data sampling they usually suffer from aliasing that can substantially degrade their performance. The nature of aliasing is well understood (e.g., Turner, 1990). Various methods for alias protection in Radon were suggested. Most popular among them imply dip-dependent low-pass filtering of the input data. A more recent approach (e.g., Herrmann et. al., 2000) applies scaling of the high-frequency components of the Radon transformed data. Here we present a theory of a scaling algorithm for alias suppression with a dip-dependent noise estimator and give synthetic and real data examples.

Introduction

The quality and resolution of the data in the Radon domain is degraded with artifacts caused by coarse offset sampling. Poor focusing of the events hampers subsequent processing. A possible way to attack aliasing is to design a frequency-selective operator for the Radon transform, i.e. incorporate a dip-dependent low-pass filter into it. A disadvantage of such filtering is attenuation of high-frequency components of the signal. Schultz and Claerbout, 1978 realized that aliasing is introduced into the slant stack due to summation across events. The Radon stacking is global, hence, along with contribution from regions of tangency spurious energy is accumulated from regions where the slant sum trajectory intercepts an event at a large angle. In case a priori information about the actual moveouts is available the aliasing problem can be well treated with fine aperture tuning: anti-alias windowing localizes the data summation gate. Such approach requires good knowledge of stacking velocities and adequacy of the hyperbolic moveout assumption.

Our approach is based on high-frequency component scaling and combines the advantages of dip filtering and local slant stacking with no need to know the moveouts of the events. Here we follow the work of Denisov and Finikov, 2001 and construct the Radon transformed data from de-aliased local slant sums. The theory of the algorithm is based on the following simple idea. Stacking an event along a slanted line that results in aliasing, produces the output signal with subsidiary peaks away from any peaks in the true spectrum. Therefore, the filter should compare the output with the input signals and prevent appearance of false peaks. The method consists of the three steps as follows.

(1) Local slant summations, (2) Application of a non-linear anti-alias scheme, (3) Construction of the global Radon from local de-aliased sums.

Method

In the first step, given the data $w(x, t)$ we perform local summations along dipping lines $t + px$ within a spatial gate $(-L, L)$ centred on a current coordinate, y , and obtain a local decomposition result:

$$d(y, p, t) = \sum_{x=-L}^L w(y-x, t+px).$$

Although the decomposition is local, dips of the tangent lines that define the summation direction do not necessarily coincide with the actual dips of events. In other words, we have to tackle the aliasing problem. So, we pass to the second step, a nonlinear anti-alias scheme

$$\tilde{d}(y, p, t) = \sum_{\tau} d(y, p, \tau) f(d(y, p, \tau), p, t - \tau).$$

We consider an assumption as follows. The low-frequency components of the signal usually are not expected to be aliased after slant summation. On the other hand, aliasing in high frequencies manifests itself in increase of amplitudes for some frequencies at some dips. Clearly, low frequencies are summated best. Therefore, if we specify a band, (ω_1, ω_2) , in the low frequency region and estimate the original signal, $w(y, t)$, energy to the output signal, $d(y, p, t)$, energy ratio within the band for every local summation dip p we will obtain a

threshold, R^p , that cannot be exceeded at any high frequency: $R^p = \frac{\int_{\omega_1}^{\omega_2} A^2_{output(p)}(\omega)d\omega}{\int_{\omega_1}^{\omega_2} A^2_{input}(\omega)d\omega}$,

where $A_{input}(\omega)$ and $A_{output(p)}(\omega)$ are amplitude spectra of the input and slant stacked signals, respectively. In other words, the constraint we impose on the high frequencies of the local slant sum is

$$R^p(\omega) \leq R^p, \text{ where } R^p(\omega) = \frac{A^2_{output(p)}(\omega)}{A^2_{input}(\omega)}.$$

The anti-alias filter, $F^p(\omega)$, is designed as

$$F^p(\omega) = \begin{cases} 1, R^p(\omega) \leq R^p \\ \frac{A_{output(p)}(\omega)}{R^p A_{input}(\omega)}, R^p(\omega) > R^p \end{cases}.$$

Besides, we introduce a restriction $F^p(\omega) \leq 1$. The filter is calculated and applied within the band $(\omega_2, \hat{\omega})$, where $\hat{\omega}$ stands for the maximum frequency of the input data.

Since the method is designed for application to pre-stack data, one of the most important problems with it is to provide noise-free amplitude spectra for both the input signal and the p -trace. If random noise is present, the spectrum energy estimator will produce a biased result. Therefore, the anti-alias algorithm should be equipped with a noise estimator to compensate for the bias. It is convenient to obtain a noise estimate with a procedure similar to the Radon decomposition. To design an unbiased estimate of $A_{output(p)}(\omega)$, we consider the result of the local slant summation with weights equal to one $(1, 1, \dots, 1)$ to be signal plus noise, as an auxiliary sum obtained with weights alternating for adjacent traces $(1, -1, \dots, 1)$ to be pure noise. The difference between them provides an unbiased signal spectrum estimate. Both sums can be calculated recursively. It is an important feature of the algorithm that the signal and noise energy estimation is carried out in a dip-dependent way. This essentially improves the performance of the scheme.

If within the local summation gate an event might be approximated with a plane wave $s(t - \alpha x)$ the amplitude spectra of the p -traces obtained with $(1, 1, \dots, 1)$ and $(1, -1, \dots, 1)$ weight functions will be

$$|P(\omega)| = \frac{1}{M} \left| S(\omega) \frac{\sin[\omega(\alpha - p)M/2]}{\sin[\omega(\alpha - p)/2]} \right| \text{ and } |Q(\omega)| = \frac{1}{M} \left| S(\omega) \frac{\cos[\omega(\alpha - p)M/2]}{\cos[\omega(\alpha - p)/2]} \right| \quad M = 2L + 1,$$

respectively. As it can be easily seen, $|P(\omega)|$ differs from $|Q(\omega)|$ only in a shift $\pi/(\alpha - p)$. Due to data sampling in x-coordinate both functions are periodic displaying aliasing peaks for high frequencies and large differential dips, i.e. large values of $\omega(\alpha - p)$. Figure 1 provides an example of the spectral functions calculated for $\alpha - p = 6$ samples per channel, $|S(\omega)| = 1$ and five traces contributing the slant sum $M = 5$.

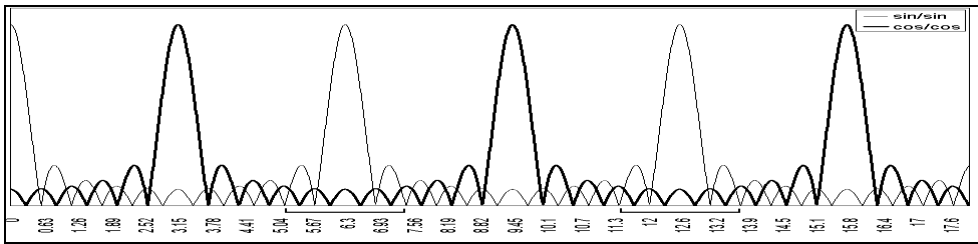


Figure 1

The maxima of $|P(\omega)|$ correspond to the minima of $|Q(\omega)|$. The zones to be corrected for aliasing are marked by brackets. The local maxima of $|Q(\omega)|$ do not hamper alias suppression since they always correspond to the local minima of $|P(\omega)|$, i.e. the zones free from aliased frequencies.

An unbiased estimate of the input signal amplitude spectrum might be obtained directly from each gather with an algorithm based on computation of cross-correlation of adjacent traces in a short sliding gate with subsequent averaging. Intensive testing on synthetic and real data proved high efficiency of this algorithm. Besides, an input signal spectrum estimate might be obtained from post-stack data.

In the last step the Radon gathers are constructed from the output of step 2:

$$W() = \sum_y \tilde{d}(y, p = \left. \frac{\partial \tau(x)}{\partial x} \right|_{x=y}, t + \tau(y)),$$

where the summation is performed along the transform trajectory $\tau(y)$.

All expressions are given in the general form, i.e. both linear and non-linear Radon can be computed with them.

For a linear transform we use $\tau(y) = py$.

The steps above describe the approach briefly and schematically and omit some non-substantial features like normalisation, etc.

Examples

We demonstrate the performance of the anti-alias scheme incorporated into a linear Radon transform on synthetic and real data. Figure 2(left) shows a simulated shot gather that contains two strong and one weak reflections. Although a dip filter was applied, on the result of a conventional Radon (Figure 2(centre)) the weak event is masked with artefacts of the strong ones. Application of both the dip filter and the anti-alias scheme enables detection of the weak event (see Figure 2(right)). Also, Figure 2 shows amplitude spectrum estimates obtained from a marked rectangular data segment in the Radon domain. Clearly, the scheme succeeded in attenuation of the false spectrum peaks. Note that a compensation filter $\sqrt{\omega}$ was applied to neither of the results

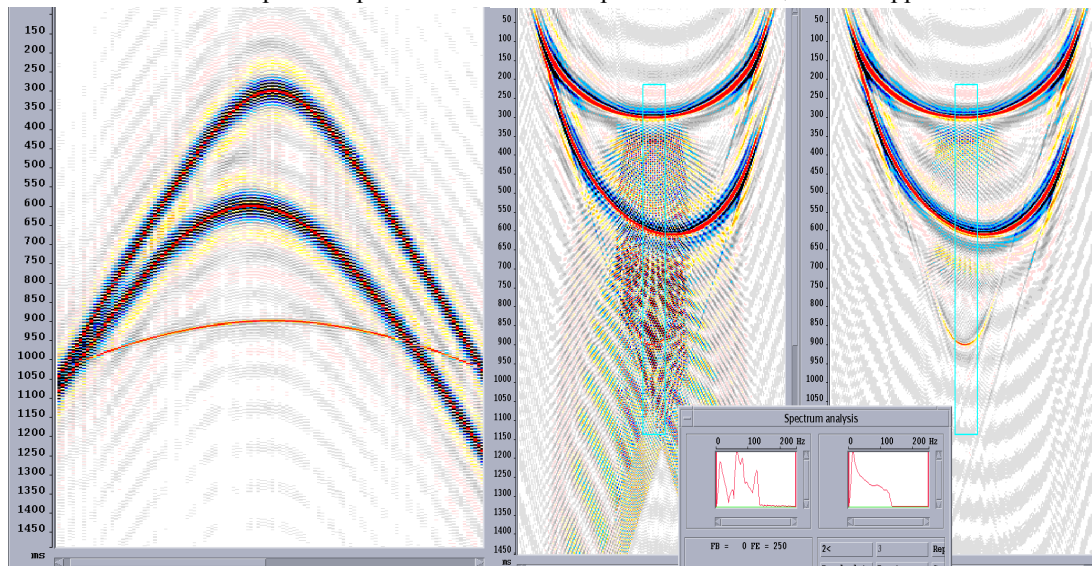


Figure 2. The input synthetic shot gather (left), output of the conventional Radon (centre), output of de-aliased Radon (right).

A marine data shot gather is given in Figure 3(left). The conventional linear Radon transform result with dip filtering is shown in Figure 3(centre). A de-aliased Radon with dip filtering is shown in Figure 3(right). In this case the scheme suppressed most of the alias noise energy providing a clear image in the Radon domain.

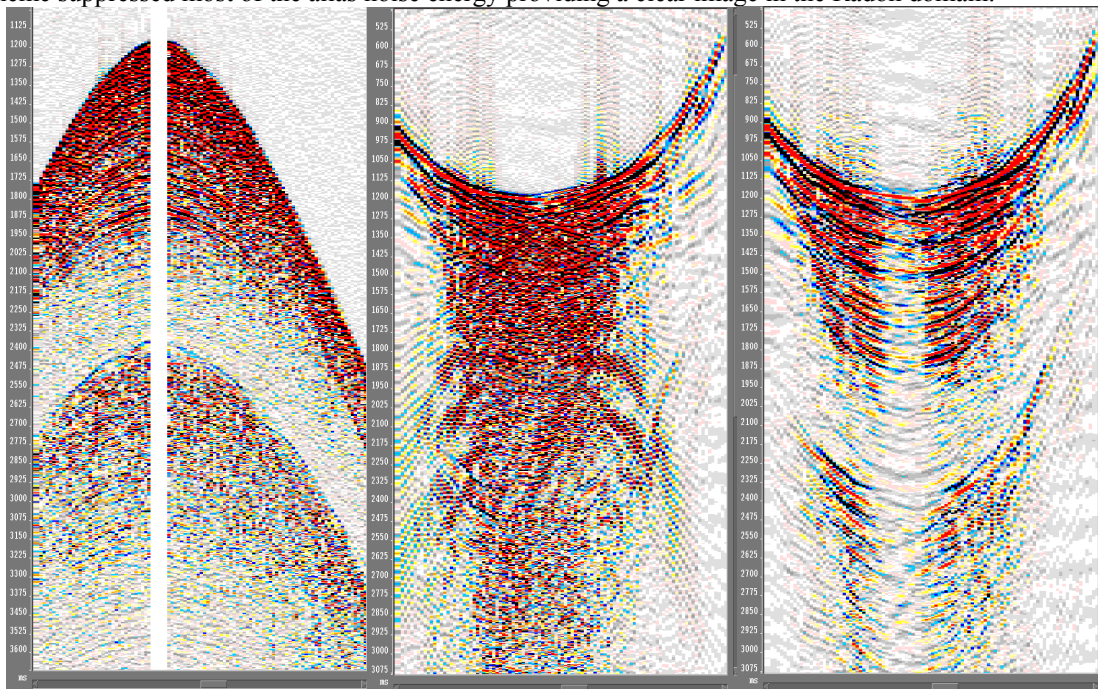


Figure 3. A real marine shot gather (left), conventional Radon transform result (centre), de-aliased Radon (right).

One of the possible applications of the de-aliased Radon is wavefield extrapolation. An example of multiple modelling obtained with alias protection is compared with that with no protection in Figure 4.

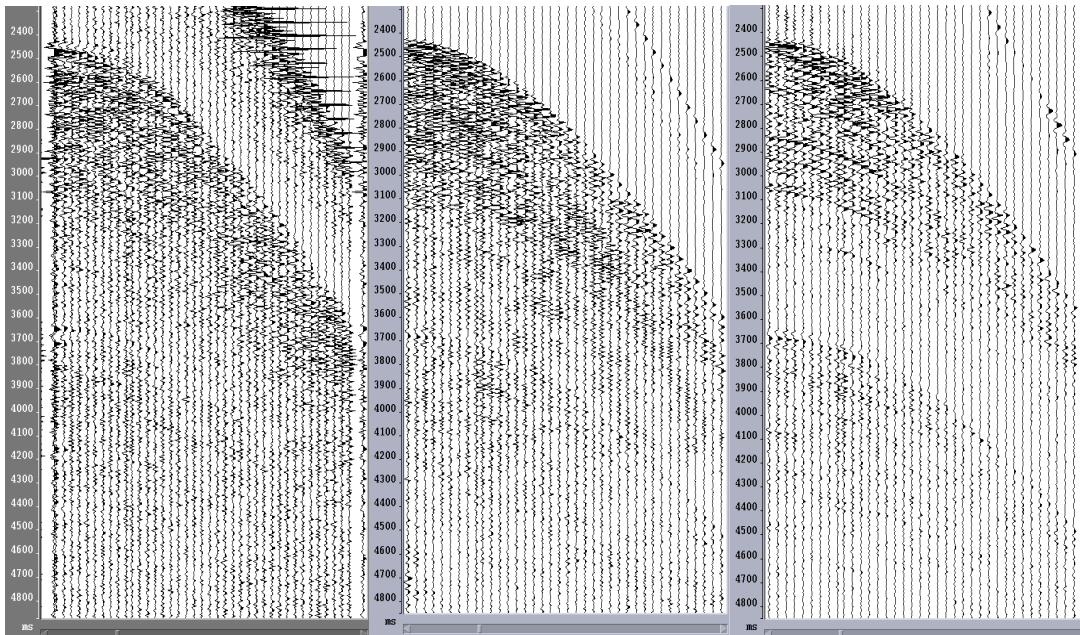


Figure 4. An original marine CMP gather (left), model of multiples obtained with the conventional Radon (centre), multiples obtained with the de-aliased Radon (right).

Clearly, the multiple modelling result shown on the right is preferable for subsequent adaptive subtraction. Besides, a simplified modification of the anti-alias scheme was successfully applied for sea-floor data processing (Lokshtanov et al., 2002).

Conclusions

This anti-alias scheme suggested shows good performance on synthetic and real data. The method is theoretically simple and relatively easy to program. Since the algorithm is based on a threshold technique, its application is safe in respect to signal preservation.

Unbiased signal spectrum estimation in a dip-dependent way provides an accurate constraint for the high-frequency components in the Radon transform domain.

Windowing of the slant summation in the first step of the three step scheme is an essential feature of the whole algorithm. Since the decomposition is local, it enables accurate correction for the distortions due to stacking across events.

The scheme is applied in the frequency domain. Therefore, it is convenient to incorporate it into the fast Radon transform.

Acknowledgments

The authors would like to thank Norsk Hydro for financial support of the research and personally Dmitri Lokshtanov for fruitful discussions.

References

- Turner, G., 1990, Aliasing in the tau-p transform and removal of spatial coherent noise: *Geophysics*, 55, 1496-1503.
 Herrmann, P., Mojesky, T., Magesan, M., and Hugonnet, P., 2000, De-aliased, High Resolution Radon transform: 70th SEG, Meeting, Expanded Abstracts, p. 1953-1956.
 Schultz, P.S., and Claerbout, J.F., 1978, Velocity estimation and downward continuation by wavefront synthesis: *Geophysics*, 43, 691-714.
 Denisov, M., and Finikov, D., 2001, Wavefield extrapolation based on the local slant stacking: EAGE 63rd meeting, paper P168.
 Lokshtanov, D., Denisov, M., and Finikov, D., 2002, Multiple suppression and datuming with an antialiased Radon transform for sea-floor data: EAGE 64th meeting.